Article

Not peer-reviewed version

IMU Networks for Trajectory Reconstruction in Logistics Applications

João Silva Sequeira *

Posted Date: 20 July 2023

doi: 10.20944/preprints202307.1375.v1

Keywords: Trajectory reconstruction; Inertial Measurement Unit; Linear Matrix Inequalities; Covariance Intersection; Target Following

Article

IMU Networks for Trajectory Reconstruction in Logistics Applications

João Silva Sequeira [1]

[1] J. Sequeira is with the Institute for Systems and Robotics, Instituto Superior Técnico, Lisbon, Portugal; joao.silva.sequeira@tecnico.ulisboa.pt

* Correspondence: joao.silva.sequeira@tecnico.ulisboa.pt

Abstract: This paper discusses the use of networks of Inertial Measurement Units (IMU) for the reconstruction of trajectories from sensor data. Logistics is a natural application domain, to verify the quality of the handling of goods. This is a mass application and the economics of logistics impose that IMUs to be used must be low cost and use basic computational devices. The approach in the paper converts a strategy from the literature, used in the multi-target following problem, to reaching a consensus in a network of IMUs. The paper presents results on how to achieve the consensus in trajectory reconstruction, along with covariance intersection data fusion of the information obtained by all nodes in the network.

Keywords: trajectory reconstruction; Inertial Measurement Unit; Linear Matrix Inequalities; covariance intersection; Target Following

1. Introduction

Logistics is a booming service industry. With the diversity of goods being transported between any two points around the world, one of the quality indicators used by logistics operators is the way goods are manipulated during their transportation. Poor handling may result in damages and/or liability costs to insurance and/or logistics operators.

In engineering terms, this amounts to analyze the trajectories the goods are subject to, i.e., the trajectories resulting from the way they are manipulated during the transportation.

The trajectory reconstruction problem is well known in, for example, the aerospace industry. Using information from IMU attached to the body of the spacecraft, its trajectory can be reconstructed using the velocity and acceleration data and assuming a good model of the spacecraft. Essentially, this amounts to an optimization problem, where the reconstructed trajectory must be such that the data it generates is close to the observed data. The literature on the problem is vast, see for instance [1] on using multiple models and Unscented Kalman Filtering (UKF) [2] on using Extended Kalman Filtering (EKF) techniques and inertial measurement data [3] on using image data, [4] on using Gaussian regression techniques and GPS data.

The extension to the logistics problem introduces additional constraints, namely, sensing must be really cheap (i.e., the quality of the accelerometers and rate-gyros is nowhere close to that used in the aerospace industry), and the rigidity of the goods is only loosely verified. For example, goods such as food or domestic appliances are often transported in cardboard boxes and hence, rigidity is valid under the assumption that handling forces are relatively small or highly localized to avoid damages. Moreover, the placement of the sensors will, in general, be made by unskilled/carefree operators which may lead to devices malfunctioning and hence redundancy, as with using multiple (similar) devices, is likely to increase the amount of usable information for trajectory reconstruction.

The vision of the paper to implement this redundancy is that of a network of low cost IMUs that can be glued-and-forgotten in typical packages (made out of cardboard, wood, plastic, metal, etc). These IMUs can be either be placed (i) forming a regular, pre-defined, pattern, with the packages specifying precise areas where to "glue" the devices, or (ii) distributed through the package arbitrarily. Placing the devices must not require any special expertise. The first scenario is possible in packages

Preprints (www.preprints.org) | NOT PEER-REVIEWED | Posted: 20 July 2023 doi:10.20944/preprints202307.1375.v1

of standardized dimensions and limits the need for calibration procedures. In the second scenario some calibration procedure may be necessary prior the start of the transportation. For the sake of simplicity, this paper assumes that the whole IMUs in the network are placed at the same point. This does not imply any lack of generality; in a real scenario, with all IMUs placed in different locations, the reconstructed trajectories would differ among them by constant homogeneous transformations.

Having multiple IMUs gathering data and combining it to reconstruct the trajectory may, in principle, improve the robustness of the solution, as (i) the amount of data increases and it may contain richer information, and (ii) redundancy helps dealing with sensor fails. Combining *a posteriori* the solutions found, from the data collected from each IMU independently of each others, e.g., using covariance intersection or some other averaging method, is a possibility and does not require exchange of information among nodes. The alternative, followed in this paper, is to have a network of nodes, each including (i) sensory information from a local IMU and (ii) communication with other distributed nodes (of similar architecture) to the exchange of information[1]. The novel approach presented here follows from a multi-target tracking problem first presented in [5], re-interpreted as a consensus generation in a network of IMUs. The motivation to use this formulation comes from the proven optimality of the framework in [5] in the context of the multi-tracking problem.

The paper is organized as follows. Section 2 illustrates a single, simulated, IMU, establishing a baseline performance for comparison with the consensus approach. Section 3 presents a quick view of the work in [5], which serves as a basis for this work, focusing on the consensus features and clarifying the re-interpretation of the key terms. Moreover, the feasibility problem, i.e., the existence of a strategy for the exchange of information such that all nodes in the network can provide estimates of the reconstruction, is discussed using the Linear Matrix Inequalities (LMI) framework. Section 4 illustrates the evolution of performance indicators of simulated nodes recovered from the network framework when the communications among them are inhibited. Section 5 presents simulation results with simple networks with 2 and 3 nodes. Section 6 discusses the improvement of the network consensus over reconstruction by independent nodes. Section 7 presents results on the fusion of the trajectories reconstructed by each node using Covariance Intersection. Finally, section 8 concludes the paper with a discussion on the feasibility of the approach and points to future research.

2. Baseline IMU

Given an arbitrary trajectory that serves as the ground truth, the corresponding linear and angular accelerations can be easily obtained if the inertia properties of the body (assumed rigid) moving over the trajectory are known. Thus, to accurately simulate the sensors to be glued to the logistics packages knowledge of the inertia properties of the package is required beforehand.

In practical terms, full knowledge about package inertia will seldom be available (though mass and the physical dimensions can be easily known *a priori* as they are the parameters that directly influence the transportation cost). Therefore, while the observations reflect the real properties of the packages, the reconstruction of the trajectories has only a limited amount of that knowledge available. However, it should be emphasized that estimation of mass/inertia properties can also be done using IMU data. This is a well known problem in aerospace industry, see for instance [6] on using recursive least squares, [7] on using continuous systems identification techniques to identify the dynamics of the Hubble telescope, [8] on using the LMI framework and formulating a least squares problem, and [9,10] on using the least squares formulation combined with S-estimators for the identification of spacecraft parameters.

The basic approach to estimate the trajectory from velocities and accelerations is to use simple integrator models. Given a trajectory expressed in terms of the position and orientation coordinates,

[1] The paper refers to a network of IMUs as these devices are the key component of the nodes.

Preprints (www.preprints.org) | NOT PEER-REVIEWED | Posted: 20 July 2023 doi:10.20944/preprints202307.1375.v1

$x, y, z, \alpha, \beta, \gamma$, assume that the corresponding signals from accelerometers and rate-gyros can be obtained from

$$\begin{aligned} \ddot{x} &= a_x \\ \ddot{y} &= a_y \\ \ddot{z} &= a_z \\ \begin{bmatrix} \dot{\alpha} \\ \dot{\beta} \\ \dot{\gamma} \end{bmatrix} &= \begin{bmatrix} 0 & -s_\alpha & c_\alpha\, c_\beta \\ s_\alpha\, c_\beta\, (c_\alpha - c_\alpha) & c_\alpha & s_\alpha\, c_\beta \\ 1 & 0 & -s_\beta \end{bmatrix}^{-1} \begin{bmatrix} \omega_x \\ \omega_y \\ \omega_z \end{bmatrix} \end{aligned} \tag{1}$$

where $a_x, a_y, a_z, \omega_x, \omega_y, \omega_z$ are the corresponding sensor outputs, i.e., linear accelerations and angular velocities, respectively. Also, s_θ, c_θ stand for $\sin(\theta)$ and $\cos(\theta)$, respectively. The purpose of these expressions is to yield a simulation tool and, without lack of generality, they implicitly assume a unit mass body. To improve realism, noise can be added to the outputs of these sensors.

2.1. Dead reckoning experiments

The purpose of these experiments is (i) to show the effects of noise when no compensation strategy is used, and (ii) to serve as baseline to compare with the network experiments. Using sensor data as obtained from (1), corresponding to some reference trajectory, and a dead reckoning model, the goal is to reconstruct the reference trajectory.

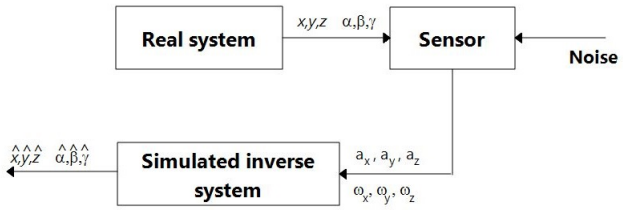

Figure 1. Dead reckoning trajectory reconstruction. Good estimates can be obtained if the model of the system is accurate and the effect of noise minimized.

Sensor uncertainties make the reconstructed trajectory deviate from the real one. Figure 2 illustrates the effects of such situations, for two levels of position noise.

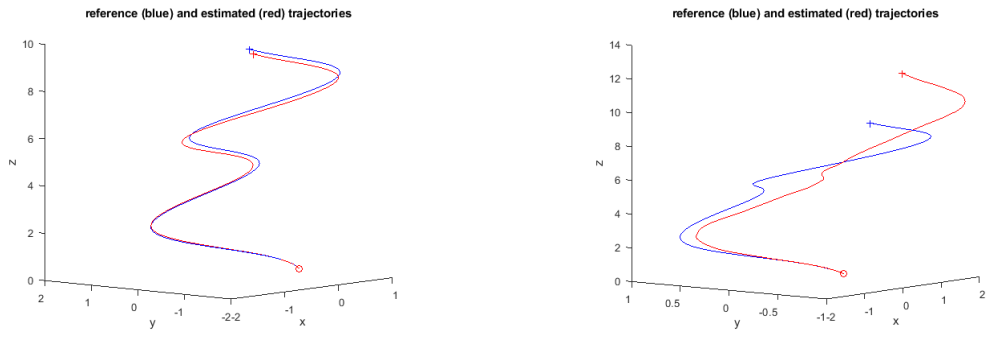

(a) Position noise $N(0, 0.1)$, Orientation noise $N(0, 0.1)$

(b) Position noise $N(0, 0.5)$, Orientation noise $N(0, 0.5)$

Figure 2. Dead reckoning test, x-y-z trajectory (orientation trajectory not shown).

From the perspective of a logistics application this simple approach may still be a valid option if disturbances are limited and only specific events are relevant to measure the quality of the handling, e.g., if the existence of strong nonsmooth/disturbances areas is required. In such cases, even if the reconstructed trajectory in the cartesian 3D space differs significantly from the real one, the presence of areas of strong disturbances can still be recognized and it is the relevant event in what concerns assessing the quality of the handling.

Preprints (www.preprints.org) | NOT PEER-REVIEWED | Posted: 20 July 2023 doi:10.20944/preprints202307.1375.v1

The existence of drifts in the observed variables is another important disturbance factor. Poor assembly of a sensor, electronics issues, are common causes of drifts. In the accelerometer, drift means that the dynamics of the acceleration is constantly integrating some value that is not being observed by the accelerometer. In the case of the rate-gyro, this means that the dynamics of the rotational velocity is constantly integrating some value that is not being directly observed by the gyro.

Figure 3 illustrates two experiments of the dead reckoning approach under constant drift conditions.

The disturbances considered affect only the linear acceleration. In the first sample they are given by

$$a_{offset_k} = a_{offset_{k-1}} + [0.05 * \text{randn}, 0, 0]$$

where *randn* stands for the usual function returning a random value with a $N(0,1)$ distribution. In the second sample all the coordinates are similarly affected by a term, $0.05 * \text{randn}$.

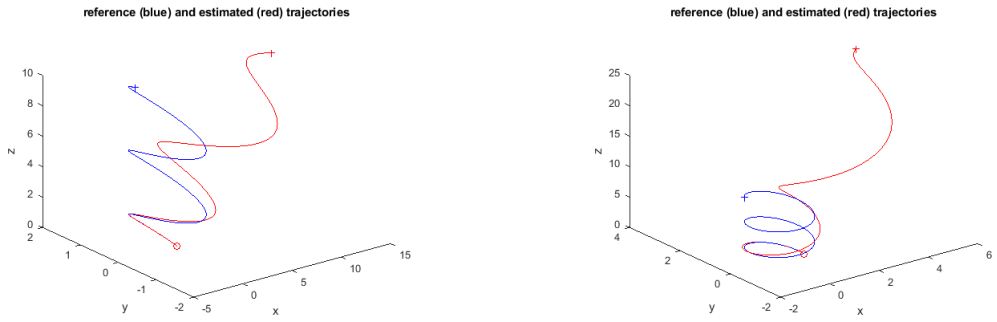

(a) Drift in the x acceleration component

(b) Drift in the x, y, z acceleration components

Figure 3. Dead reckoning experiment, spiral x-y-z trajectory, under drift conditions (Wiener process)

This is an example where the estimated trajectory is too different from the original one. However, depending on specific requirements of the logistics application, drift disturbances may not be an issue, e.g., as mentioned above if the purpose is the detection of harsh handling. Clearly, drifts are highly relevant if accurate trajectory reconstruction is required, which is the focus of the remainder of the paper.

3. Background

This paper adopts the formulation from [5], developed in the context of a multi-target tracking problem with targets and measurements assumed to have a one-to-one relation. The notation follows the usual form of the continuous-discrete (CD) extended Kalman framework (see for instance [11] for a critical comment and implementation issues of this form), with the prediction stage for the i-th IMU node given by (see also [12] for a face-off between five different formulations),

$$\begin{aligned} x^i_{k|k-1} &= f^i_{k-1}\left(x^i_{k-1|k-1}\right) \\ z^i_k &= h^i_k\left(x^i_{k|k-1}\right) \\ P^i_{k|k-1} &= F^i_{k-1} P^i_{k-1|k-1} \left(F^i_{k-1}\right)^T + Q^i_{k-1} \end{aligned} \tag{2}$$

where F is the Jacobian of f, and the modified update stage,

Preprints (www.preprints.org) | NOT PEER-REVIEWED | Posted: 20 July 2023 doi:10.20944/preprints202307.1375.v1

$$S_k^i = H_k^i \, P_{k|k-1}^i \left(H_k^i\right)^T + R_k^i \tag{3}$$

$$K_k^i = P_{k|k-1}^i \left(H_k^i\right)^T \left(S_k^i\right)^{-1} \tag{4}$$

$$x_{k|k}^i = x_{k|k-1}^i + K_k^i \, \tilde{z}_k^i \tag{5}$$

$$P_{k|k}^i = P_{k|k-1}^i - K_k^i \left(1 - \beta_0^i\right) S_k^i \left(K_k^i\right)^T + K_k^i \, \overline{P}_k^i \left(K_k^i\right)^T \tag{6}$$

where H is the Jacobian of h, and with the networking and consensus being expressed through the measurement uncertainties,

$$\overline{P}_k^i = \sum_{j=1}^{M_k} \beta_j^i \, \tilde{z}_{j,k}^i \left(\tilde{z}_{j,k}^i\right)^T - \tilde{z}_k^i \left(\tilde{z}_k^i\right)^T \tag{7}$$

using M_k measurements $\tilde{z}_{j,k}^i$ (received by the i-th IMU from the j-th IMU, i.e., the i-th IMU is connected to M_k other IMUs) and with the weighted innovations,

$$\begin{aligned} \tilde{z}_k^i &= \textstyle\sum_{j=1}^{M_k} \beta_j^i \left(z_{j,k}^i - \hat{z}_k^i\right) \\ \tilde{z}_{j,k}^i &= z_k^i - \hat{z}_{j,k}^i \end{aligned} \tag{8}$$

where β_j^i is the weight expressing the relevance of measurement from node j to the estimate of the measurement by node i, β_0^i is the weight expressing the relevance of poor measurements ($\beta_0^i \to 1$ amounts to reducing the norm of $P_{k|k}^i$, forcing the covariance to decrease even if poor measurements are being fed into the system), and $\hat{z}_k^i$, the estimate of the measurement of the i-th node at instant k, that is, $\hat{z}_k^i = h_k^i \left(x_{k|k-1}^i\right)$, and $z_{j,k}^i$, the actual measurement of node j at instant k reaching the i-th IMU.

The topology of the network is assumed fixed. In [5], the β_j^i parameters were interpreted in terms of a marginal probability of association between node j and target i. The β_0^i is used to quantify misdetection of a target (1/0 for misdetected/detected). However, for the purpose of this paper, this interpretation is not useful as the association between nodes and measurements can be known a priori. Instead, these parameters can be seen as (i) the communications protocol (as in consensus problems), and (ii) scaling weights for the measurements. Also, as in the original problem, the number of measurements, M_k, can vary along time (or measurement scans) k.

The formulation from [5] is, essentially, an EKF with a modified update of the covariance matrix (through the β_0 factor that scales the innovation residual covariance, (3), and a weighted combination of the innovations from the whole network weighted by the β_j^i. Also, (6), dumps the term explicit in the noise $K_k^i \, R_k^i \, \left(K_k^i\right)^T$, and the symmetric term $\left(K_k^i H_k^i\right)^T + K_k^i H_k^i$ affecting $P_{k|k-1}^i$ in the CD formulation of the EKF.

This innovates relative to the CD-EFK procedure in that the covariance of each unit now has feedback from the innovations produced by the network. Moreover, the tuning "knob" R_k^i in the CD-EKF formulation is now replaced with the β_j^i and β_0^i parameters. These can also be seen as the mediators/protocol/sacling factors between the nodes.

For the sake of readability, the expression for the covariance update in the CD-EKF formulation and a re-writing of (6) to highlight the differences to the CD-EKF covariance update equation, is presented below.

Preprints (www.preprints.org) | NOT PEER-REVIEWED | Posted: 20 July 2023 doi:10.20944/preprints202307.1375.v1

$$\begin{aligned} P^i_{k|k} &= \left(I - K^i_k\, H^i_k\right)\, P^i_{k|k-1}\, \left(I - K^i_k\, H^i_k\right)^T + K^i_k\, R^i_k\, \left(K^i_k\right)^T \\ &= P^i_{k|k-1} + K^i_k\, S^i_k\, \left(K^i_k\right)^T - K^i_k\, H^i_k\, P^i_{k|k-1} - P^i_{k|k-1}\, \left(K^i_k\, H^i_k\right)^T \end{aligned} \tag{9}$$

The renewed one, where $\tilde{z}_{j,k}$ and $\tilde{z}^i_{j,k}$ are $N \times M_k$ matrices is,

$$\begin{aligned} P^i_{k|k} &= P^i_{k|k-1} - K^i_k\, S^i_k\, \left(K^i_k\right)^T + \\ &+ K^i_k \left(\sum_{j=1}^{M_k} \beta^i_j\, \tilde{z}^i_{j,k}\, \left(\tilde{z}^i_{j,k}\right)^T\right) \left(K^i_k\right)^T - K^i_k\, \tilde{z}^i_k\, \left(\tilde{z}^i_k\right)^T\, \left(K^i_k\right)^T + \beta^i_0\, K^i_k\, S^i_k\, \left(K^i_k\right)^T \end{aligned} \tag{10}$$

The first two terms on the righthand side of (10) are also present in (9). The third and fourth terms, account for the network exchanges, is the additional 'tuning knob". The fifth term dampens the second term and provides additional control.

The convergence of (10) can be achieved by careful selection of β^i_0 and β^i_j, namely ensuring that $P^i_{k|k}$ is a contracting sequence converging to some fixed point (see [13]). This means

$$\exists k_0 > 0,\, \alpha > 0,\, \gamma > 0\, :\, \forall k > k_0,\, \left\| P^i_{k|k} - P^i_{k|k-1} \right\| \leq \alpha\, e^{-\gamma\,(k-k_0)}$$

or, alternatively,

$$\exists k_0 > 0,\, \alpha > 0,\, \gamma > 0\, :\, \forall k > k_0,$$

$$\left\| -(1-\beta^i_0) K^i_k\, S^i_k\, \left(K^i_k\right)^T + \sum_{j=1}^{M_k} \beta^i_j \left(K^i_k\, \tilde{z}^i_{j,k}\, \left(\tilde{z}^i_{j,k}\right)^T\, \left(K^i_k\right)^T\right) - K^i_k\, \tilde{z}^i_k\, \left(\tilde{z}^i_k\right)^T\, \left(K^i_k\right)^T \right\| \leq \alpha\, e^{-\gamma\,(k-k_0)}$$

or, in a more compact form to highlight the terms involved in the consensus, with $A^i_k = (1 - \beta^i_0) K^i_k\, S^i_k\, \left(K^i_k\right)^T$, $C^i_k = K^i_k\, \tilde{z}^i_k\, \left(\tilde{z}^i_k\right)^T\, \left(K^i_k\right)^T$, and $F^i_{j,k} = K^i_k\, \tilde{z}^i_{j,k}\, \left(\tilde{z}^i_{j,k}\right)^T\, \left(K^i_k\right)^T$,

$$\exists k_0 > 0,\, \alpha > 0,\, \gamma > 0\, :\, \forall k > k_0,$$
$$\left\| -A^i_k - C^i_k + \sum_{j=1}^{M_k} \beta^i_j\, F^i_{j,k} \right\| < \alpha\, e^{-\gamma\,(k-k_0)}.$$

At each time step a new solution must be produced so that the convergence of the covariance matrix can be controlled. This means that (i) the consensus will be adjusting over time, as the β^i_j will (in general) be changing, and (ii) tradeoff values for α, γ (that can be constant over time) has to be selected. However, one must ensure that the α, γ can be made unique during the whole duration of the trajectory, despite the changes in the β^i_j.

Making,

$$Z^i_k = \frac{1}{\alpha} e^{\gamma(k-k_0)} \left(-A^i_k - C^i_k + \sum_{j=1}^{M_k} \beta^i_j\, F^i_{j,k}\right)$$

the solution of

$$\left\| Z^i_k \right\| < 1$$

Preprints (www.preprints.org) | NOT PEER-REVIEWED | Posted: 20 July 2023 doi:10.20944/preprints202307.1375.v1

can be obtained using the LMI form (see for instance [14], pp. 7-8, on computing maximum singular values) as,

$$\begin{bmatrix} I & Z_k^i \\ \left(Z_k^i\right)^T & I \end{bmatrix} > 0, \tag{11}$$

The complete solution for the convergence of (10) requires an additional LMI that imposes the positive definiteness of $P_{k|k}^i$ given that $P_{k|k-1}^i$ is assumed positive definite,

$$P_{k|k-1}^i - A_k^i - C_k^i + \sum_{j=1}^{M_k} \beta_j^i F_{j,k}^i \succ 0$$

or, more compactly, with $D_k^i = P_{k|k-1}^i - A_k^i - C_k^i$,

$$D_k^i + \sum_{j=1}^{M_k} \beta_j^i F_{j,k}^i \succ 0 \tag{12}$$

Therefore, if (11) and (12), with the β^i variables, are both feasible at each time step, k, for some choice of β_j^i, then there is a consensus solution to the network, from the point of view of the i-th node, which ensures the convergence of $P_{k|k}^i$. **A solution for the full network requires the feasibility of the above LMI problems for all the nodes.**

LMI feasibility can be tested by multiple algorithms, from general ones, [15,16] on ellipsoid algorithms, to specific ones, [17] for large and sparse LMIs or [18] on stochastic algorithms. Several software packages to solve LMIs are available, i.e., the Scilab based LMITOOL,[19], the Matlab based YALMIP, [20], and the Matlab LMI toolbox.

These LMI problems are non-convex (the presence of the affine term in (12) is enough to make it non-convex) and hence finding optimal parameters using standard LMI solvers is, in general, an issue. Relaxation techniques are commonly used to solve non-convex problems. and obtain either good solutions or pseudo-solutions from which approximations to the good ones can be derived (see, for instance, [21–23]). The approach proposed here uses a basic form of relaxation, consisting in scaling some terms until a solution can be found.

4. Simulation experiments

Making $\beta_0^i = 0$ and $\beta_j^i = 1$, if $i = j$, and 0, otherwise, then $\tilde{z}_k^i = \tilde{z}_{j,k}^i$ for $j = i$, recovering a set of isolated nodes and

$$E_k^i \equiv P_{k|k-1}^i - K_k^i S_k^i \left(K_k^i\right)^T > 0 \tag{13}$$

and the convergence condition becomes,

$$\left\| \frac{1}{\alpha} e^{\gamma(k-k_0)} \left(-K_k^i S_k^i \left(K_k^i\right)^T \right) \right\| < 1. \tag{14}$$

Given that all the matrices in (13) are norm-bounded then the 2nd condition can always be verified for large enough α and small enough γ.

The noise covariance R_k^i bounds the definiteness of (13) (in the best possible scenario $R_k^i = 0$; in general this is not a free parameter as it must be chosen in connection with the sensors, though it can also act as a tuning knob to some extent). The matrix S_k^i is, by construction, always positive definite and hence the quadratic term $K_k^i S_k^i \left(K_k^i\right)^T$ is also positive definite. By introducing a scale factor

Preprints (www.preprints.org) | NOT PEER-REVIEWED | Posted: 20 July 2023 doi:10.20944/preprints202307.1375.v1

$\xi_k^i \in [-1,1]$ in K_k^i , the LMI (14) dominates that in (13), i.e., the set of solutions $P_{k|k-1}^i$ of (14) contains those of (13) (see [24] for detailed analysis and results related to LMI dominance).

Given the scaled expression

$$P_{k|k-1}^i - \left(\xi_k^i\right)^2 K_k^i \, S_k^i \, (K_k^i)^T > 0,$$

as $\xi_k^i \to \pm 1$ the solution $P_{k|k-1}^i$ converges to that of the unscaled expression. Also, as $\xi_k^i \to 0$, $P_{k|k} \to P_{k|k-1}^i$, which is by construction positive definite.

Given the low complexity of the scaled expression, its feasibility relative to the ξ_k^i parameter can be obtained from the eigenvalues/eigenvectors of the matrix

$$G_k^i \equiv P_{k|k-1}^i \left(\xi_k^i\right)^{-2} \left(K_k^i \, S_k^i \, (K_k^i)^T\right)^{-1}$$

Positiveness of all eigenvalues means $G_k^i > 0$. As the ξ_k^i varies, the eigenvalues of the relaxed matrix are linearly related to those of G_k^i.

Figure 4 shows an example of the evolution of the eigenvalues using $\xi_k^i = 1$

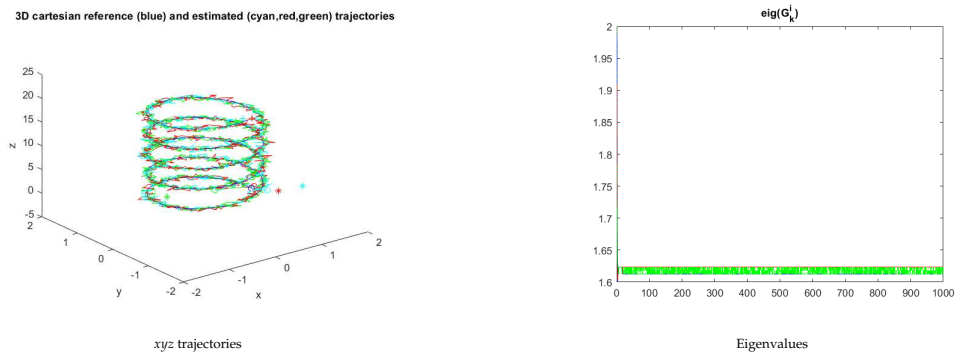

Figure 4. Trajectories and eigenvalues evolution for 3 independent nodes. The positive definiteness of the G_k^i matrix is clear.

As expected, the quality of this solution, using the EKF, is clearly superior to that in the example on dead reckoning.

Whenever the nodes are not independent and the network must reach a consensus the feasibility must be checked directly using (11) and (12).

5. Network consensus experiments

Figure 5 shows the 3D space trajectories for the 2 nodes operating independently and as a network. All IMUs assumed time-synchronized, i.e., the simulation loop time is the same for all of them. For the independent nodes test, $\beta_0^i = 0$, $i = 1,2$, $\beta_1^1 = 1, \beta_2^1 = 0, \beta_1^2 = 0, \beta_2^2 = 1$. For the networked nodes test, $\beta_0^i = 0.01$, $i = 1,2$, $\beta_1^1 = 0.6, \beta_2^1 = 0.4, \beta_1^2 = 0.4, \beta_2^2 = 0.6$. Any of the IMU trajectories can be used for reconstruction purposes.

Preprints (www.preprints.org) | NOT PEER-REVIEWED | Posted: 20 July 2023 doi:10.20944/preprints202307.1375.v1

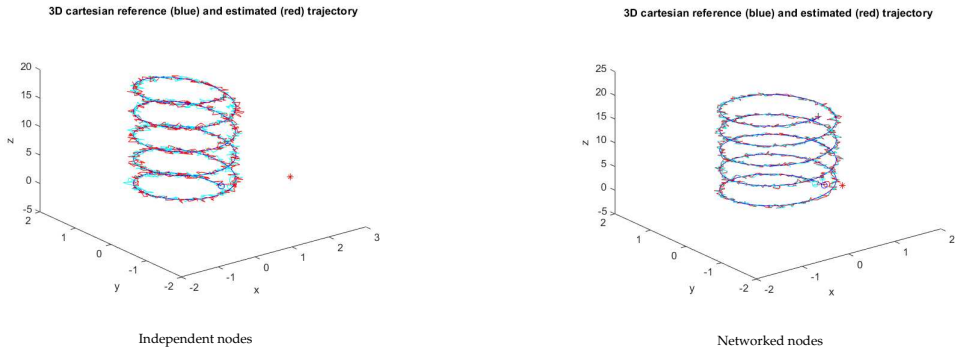

Figure 5. Samples of the two node network xyz trajectories.

Figure 6 shows the evolution of the 2-norm of the xyz trajectory and of the respective mean. Clearly, the mean error when the nodes operate cooperatively is lower than when operating independently.

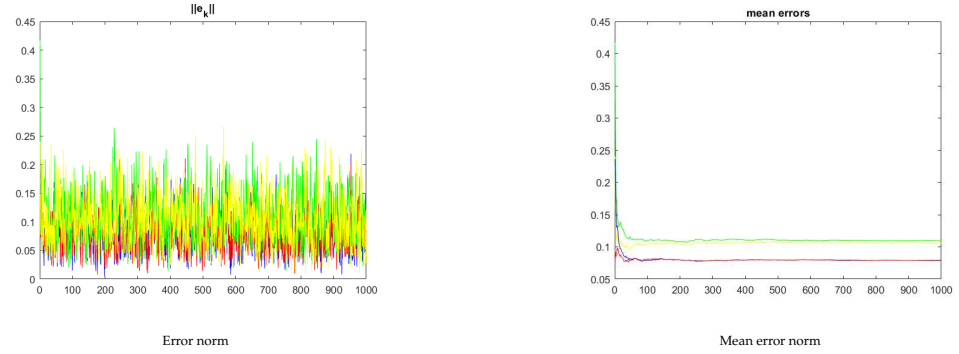

Figure 6. Two node error evolution for the samples in figure 5 (the red/blue curves refer to the networked nodes; the yellow/green curves in the righthand plot refer to the independent nodes under no-consensus).

Figures 7 and 8 show a similar experiment with 3 nodes. For the independent nodes test, $\beta_0^i = 0, i = 1,2,3$, $\beta_1^1 = 1, \beta_1^2 = 0, \beta_2^1 = 0, \beta_2^2 = 1, \beta_2^3 = 0, \beta_3^1 = 0, \beta_3^2 = 0, \beta_3^3 = 1$. For the networked nodes test, $\beta_0^i = 0.01, i = 1,2,3$, $\beta_1^1 = 0.7, \beta_2^1 = 0.01, \beta_3^1 = 0.01, \beta_1^2 = 0.01, \beta_2^2 = 0.7, \beta_3^2 = 0.01, \beta_1^3 = 0.01, \beta_2^3 = 0.01, \beta_3^3 = 0.8$.

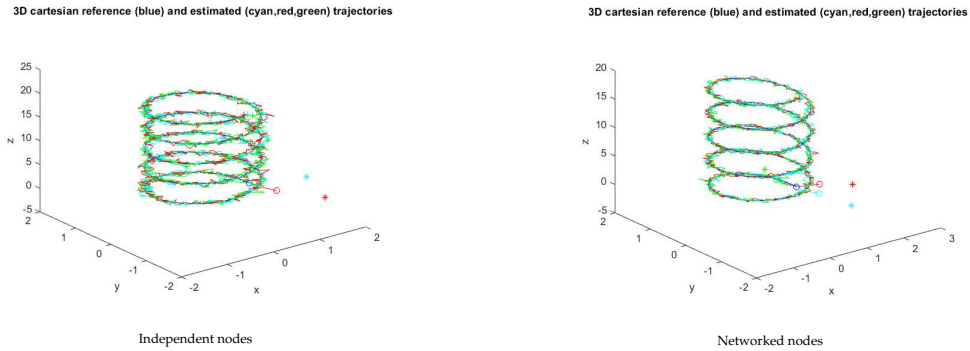

Figure 7. Samples of the three node network xyz trajectories.

For the three-node network the mean error of the xyz trajectory of the networked nodes is also lower than the error for the independent nodes.

Preprints (www.preprints.org) | NOT PEER-REVIEWED | Posted: 20 July 2023 doi:10.20944/preprints202307.1375.v1

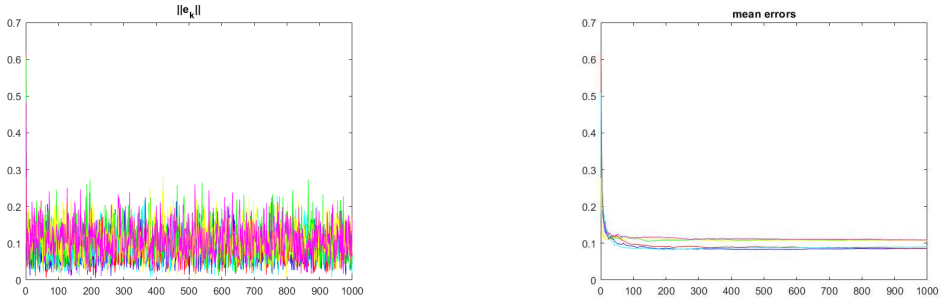

Error norm Mean error norm

Figure 8. Three node network error evolution for the sample in Figure 7 (the red/blue/cyan curves refer to the networked nodes; the yellow/green/magenta curves in the righthand plot refer to the independent nodes under no-consensus).

The evolution of the feasibility conditions, i.e., (11) and (12), is shown in Figure 9.

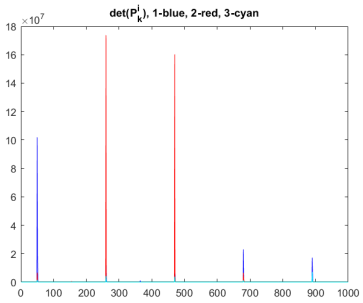

Figure 9. Feasibility evolution ($\alpha = 1000, \gamma = 10^{-5}$) for the 3 node experiment.

From a practical perspective, if during a reconstruction the LMI problem returns unfeasible then simply use one of the independent units as solution.

6. Networking for improvement over independent nodes

As seen before, the feasibility of a network can be tied to a LMI. Also, the experiments in the previous section empirically show that networks have and advantage over independent nodes. The purpose of this section is to demonstrate this advantage, i.e., the difference between the tracking errors obtained in the networked and independent versions,

$$e_k^i = \left\| e_k^{inet} \right\| - \left\| e_k^{ind} \right\| = \left\| r - x_{k|k}^{inet} \right\| - \left\| r - x_{k|k}^{ind} \right\|$$
$$= \left\| r - x_{k|k-1}^{inet} + K_k^{inet} \tilde{z}_k^{inet} \right\| - \left\| r - x_{k|k-1}^{ind} + K_k^{ind} \tilde{z}_k^{ind} \right\|, \quad (15)$$

where r is the reference trajectory, $x_{k|k}^{inet}$ is the trajectory reconstructed by a network, and $x_{k|k}^{ind}$ is a trajectory reconstructed by one node operating independently, verifies the averaging relation

$$\exists N : n > N, \frac{1}{n} \sum_{k=1}^{n} e_k^i < 0 \quad (16)$$

For a discrete, time varying, linear system, Lemma 3.1 in [25] states that $P_{k|k}^{ind}$ is bounded above and below, i.e., $\exists \mu_l, \mu_u > 0 : \mu_l I < P_{k|k}^{ind} < \mu_u I$. S_k^{ind} is a linear operator on P^{ind} and hence it is also bounded above and below. K_k^{ind} is also bounded as depends on the bounded P^{ind} and on $(S_k^{ind})^{-1}$

Preprints (www.preprints.org) | NOT PEER-REVIEWED | Posted: 20 July 2023 doi:10.20944/preprints202307.1375.v1

which is also upper and lower bounded. Therefore, x_k^{ind} is bounded and, also, the whole rightmost term in (15) can be written as

$$L_i \mathbb{I} < r - x_{k|k-1}^{ind} + K_k^{ind} \tilde{z}_k^{ind} < L_s \mathbb{I}$$

for some $L_i, L_s > 0$ and $\mathbb{I}$ a suitable identity matrix.

Applying a 2-norm on both sides of an inequality preserves the inequality, as this norm is monotone [26], and the righthand term can thus be assumed to be a bounded function,

$$L_i < \left\| r - x_{k|k-1}^{ind} + K_k^{ind} \tilde{z}_k^{ind} \right\| < L_s$$

The leftmost term in (15) is a function of the β_j^i parameters. Without loosing generality, one can represent this term as,

$$\left\| r - x_{k|k-1}^{inet} + K_k^{inet} \tilde{z}_k^{inet} \right\| \equiv \| r - g(\beta) + \beta f(\beta) \|$$

with $f(\cdot), g(\cdot)$ adequate functions. Therefore, (15) can be written as,

$$\| r - g(\beta) + \beta f(\beta) \| - L_s < e_k^i < \| r - g(\beta) + \beta f(\beta) \| - L_i \tag{17}$$

Under the LMI feasibility conditions, $f(\cdot)$ and $g(\beta)$ are bounded and hence by selecting small enough β constants the rightand side of (17) approaches

$$\| r - g(\beta) \| - L_i \tag{18}$$

The feasibility of the LMI problem ensures the asymptotic convergence of $g(\beta) \equiv x_{k|k-1}^i \to x_{k|k}^i$ and hence it is clear that, if the networked version converges to the reference trajectory r, the e_k^i are negative.

The consensus approach can also be beneficial in case of structured unmodelled disturbances, as in the case of unmodelled drift in the sensors. From Figure 10, the consensus approach retains the good property of low mean error when compared with the nonconsensus approach.

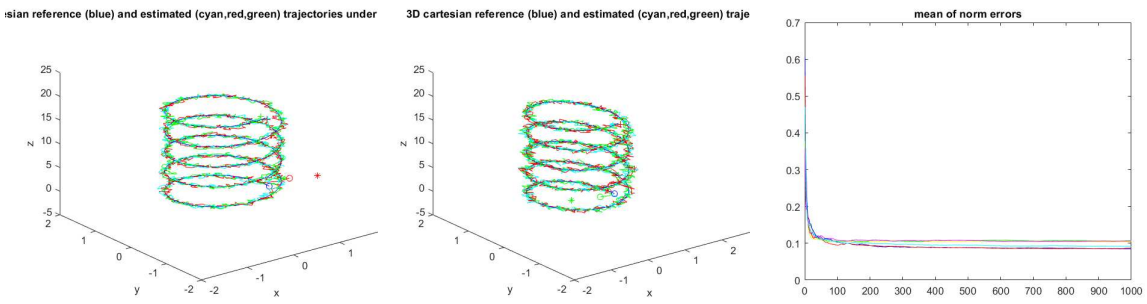

(a) Network with connected nodes (b) Network with independent (non-connected) nodes (c) Mean error in the x, y, z trajectory

Figure 10. A 3 node network with all nodes subject to unmodelled drift (the red/blue/cyan curves refer to the networked nodes; the yellow/green/magenta curves in the righthand plot refer to the independent nodes under no-consensus).

Figure 11 illustrates the performance in the case of a piecewise linear (2 trunks) reference trajectory. As before the mean error property is verified.

Preprints (www.preprints.org) | NOT PEER-REVIEWED | Posted: 20 July 2023 doi:10.20944/preprints202307.1375.v1

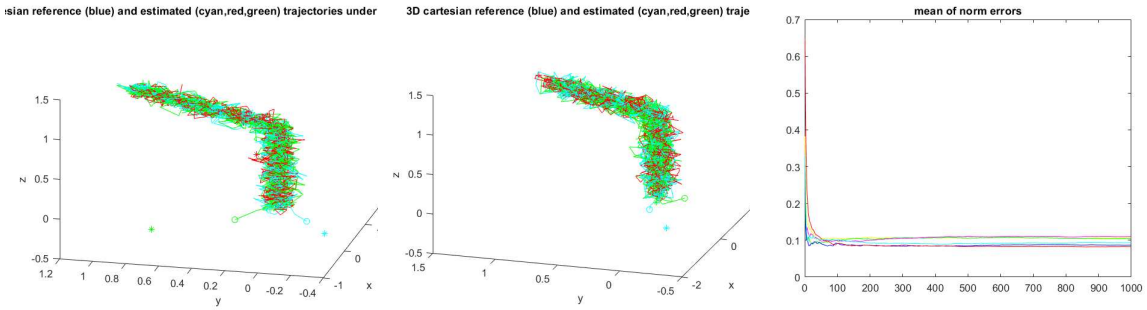

(a) Network with connected nodes (b) Network with independent (non-connected) nodes (c) Mean error in the x, y, z trajectory

Figure 11. A 3 node network with all nodes subject to unmodelled drift reconstructing a piecewise linear reference trajectory (the red/blue/cyan curves refer to the networked nodes; the yellow/green/magenta curves in the righthand plot refer to the independent nodes under no-consensus).

7. Network fusion using covariance intersection

The framework above leads to each IMU producing its own estimate, each of which better than the independent estimates. A single estimate can be obtained by applying the covariance intersection procedure [27]. Figure 12 shows the resulting trajectories for the spiral reference trajectory in the case of 2 and 3 nodes, respectively. In both cases a median filter with a 20 samples sliding window is used to smooth the output of the fusion stage. In this example, the fusion of the 3 nodes yields a smaller tracking error trend when filtered.

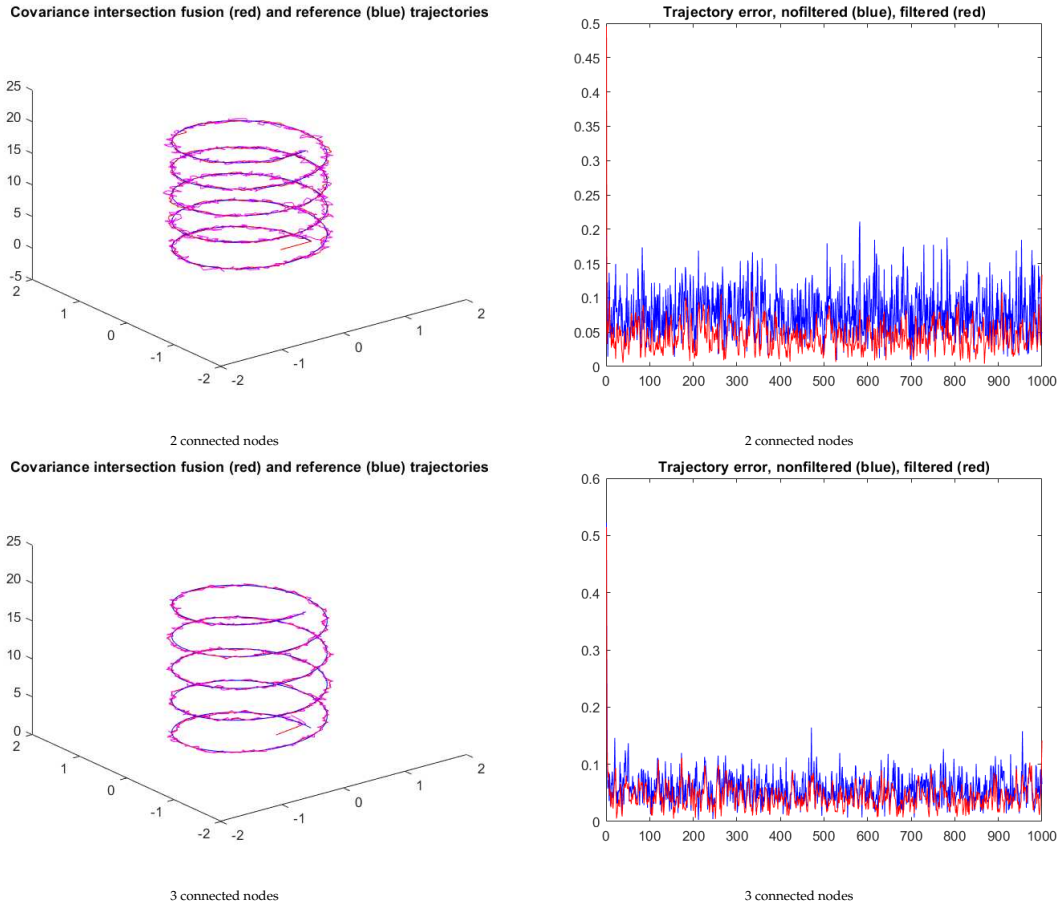

Figure 12. Trajectories and tracking errors resulting for fusion using covariance intersection ($\omega = 0.5$ in both scenarios). The blue and red curves correspond to the unfiltered and filtered stages, respectively.

8. Conclusions

The paper presented a formulation for networks of IMUs, extending a representation of the multi-target problem discussed in the literature. Feasibility conditions are discussed based on the feasibility of LMIs modeling the network. Moreover, the network with consensus version (with the nodes exchanging information among them) is shown to have an edge over the non-consensus network (i.e., with independent nodes).

Future work may involves multiples research directions. A natural evolution is the testing of alternative formulations for the EKF, e.g., the discrete formulation (which, being computationally simpler may lead to numerical problems). Also, more complex protocols need to be tested and stronger connections with the consensus theory investigated. Essentially this amounts to replace the β_j^i by adequate functions, able to shape the interchange of information among nodes.

As referred in the introduction, the rigidity assumption in the relative positioning of the IMUs is likely not to hold permanently. Rigidity criteria that can be used to determine performance bounds of the consensus approach will be a key research topic in this framework.

In the paper it is implicitly assumed that data is acquired, synchronously, and immediately processed for reconstruction. However, it should be emphasized that data acquisition and reconstruction can occur sequentially in time, i.e., data is acquired during the traveling, after which it can be downloaded and fed into the reconstruction stage. Moreover, this decoupled strategy allows the testing of different parameters for reconstruction. Also, synchronicity in data acquisition is likely not to hold for the whole duration of a mission (e.g., due to mishandling of packages which can damage the devices, intrinsic failures, electronics interferences, etc) and hence strategies to minimize the effect of missing data are to be investigated.

The advantage of combining covariance intersection and consensus was illustrated in the simple example above, when data is synchronized. Additional testing including asynchronous data scenarios, e.g., as in [28,29], is scheduled for future work.

Funding: This work was partially supported by project LARSyS-FCT Project UIDB/50009/2020.

Data Availability Statement: All software available on reasonable request to the author.

Conflicts of Interest: The author declares no conflicts of interest.

Abbreviations

The following abbreviations are used in this manuscript:

IMU	Inertial Measurement Unit
LMI	Linear Matrix Inequality
EKF	Extended Kalman Filter
CD-EKF	Continuous-Discrete Extended Kalman Filter

References

1. Huang, P.; Zhang, C.; Li, H.; Shi, F. Research on Real-Time Reentry Trajectory Reconstruction Base on Multiple Model. In Proceedings of the Procs of the 40th Chinese Control Conference, 2021. July 26-28, Shanghai, China.
2. Karlgaard, C.; Tartabini, P.; Blanchard, R.; Kirsch, M.; Toniolo, M. Hyper-X Post-Flight-Trajectory reconstruction. *Journal of Spacecraft and Rockets* **2006**, *43*. https://doi.org/10.2514/1.12733.
3. Liu, J.; Ren, X.; Yan, W.; Li, C.; Zhang, H.; Jia, Y.; Zeng, X.; Chen, W.; Gao, X.; Liu, D.; Tan, X.; Zhang, X.; Ni, T.; Zhang, H.; Zuo, W.; Su, Y.; Wen, W. Descent trajectory reconstruction and landing site positioning of Chang'E-4 on the lunar farside. *Nature Communications* **2019**, *10*.
4. Takahashi, Y.; Saito, M.; Oshima, N.; Yamada, K. Trajectory reconstruction for nanosatellite in very low Earth orbit using machine learning. *Acta Astronautica* **2022**, *194*, 301–308.
5. He, S.; Shin, H.; Tsourdos, A. Distributed Joint Probabilistic Data Association Filter with Hybrid Fusion Strategy. *IEEE Transactions on Instrumentation and Measurement* **2019**.

6. Wilson, E.; Lages, C.; Mah, R. On-line, gyro-based, mass-property identification for thruster-controlled spacecraft using recursive least squares. In Proceedings of the Proc. 2002 45th Midwest Symposium on Circuits and Systems (MWSCAS-2002), 2002. 4-7 august, Tulsa, Ok, USA.
7. Anthony, T.; Andersen, G. On-Orbit Modal Identification of the Hubble Space Telescope. In Proceedings of the Proc. American Control Conference, 1995. June, Seattle, Washington.
8. Keim, J.; Açıkmeşe, B.; Shields, J. Spacecraft inertia estimation via constrained least squares. In Proceedings of the Proc. IEEE Aerospace Conference, 2006. 4-11 March, Big Sky, MT, USA, https://doi.org/10.1109/AERO.2006.1655995.
9. Milhano, T.; Sequeira, J.; Di Sotto, E. Using S-estimators in Parameter Identification. In Proceedings of the Proc. 16th Internationl Conference on Information Fusion (Fusion 2013), 2013. 9-12 July, Istanbul, Turkey.
10. Milhano, T.; Sequeira, J.; Di Sotto, E. Spacecraft Parameter Identification Using S-Estimators. In Proceedings of the Proc. 9th International Conference on Guidance, Navigation & Control Systems (GNC 2014), 2014. 2-6 June, Porto, Portugal.
11. Guihal, J.; Auger, F.; Bernard, N.; Schaeffer, E. Efficient Implementation of Continuous-Discrete Extended Kalman Filters for State and Parameter Estimation of Nonlinear Dynamic Systems. *IEEE Transactions on Industrial Informatics* **2022**, *18*, 3077–3085.
12. Salau, N.; Secchi, A.; Trierwieler, J. Five Formulations of Extended Kalman Filter: Which is the best for D-RTO? 17th European Symposium on Computer Aided Process Engineering – ESCAPE17; Plesu, V.; Agachi, P., Eds. Elsevier B.V., 2007.
13. Lohmiller, W.; Slotine, J. On Contraction Analysis for Nonlinear Systems - Analyzing stability differentially leads to a new perspective on nonlinear dynamic systems, 1997.
14. Boyd, S.; El Ghaoui, L.; Feron, E.; Balakrishnan, V. *Linear Matrix Inequalities in System and Control Theory*; SIAM - Society for Industrial and Applied Mathematics, Philadelphia, 1994.
15. Vandenberghey, L.; Balakrishnan, V. Algorithms and Software for LMI Problems in Control. In Proceedings of the Procs. IEEE International Symposium on Computer-Aided Control System Design, 1996. Dearborn, Michigan.
16. Im, K.H.; Baang, D. Optimized ellipsoid algorithm for LMI feasibility problems. *International Journal of Control, Automation and Systems* **2014**, *12*, 915–917.
17. Zhang, R.; Lavaei, J. Efficient Algorithm for Large-and-Sparse LMI Feasibility Problems. 2018 IEEE Conference on Decision and Control (CDC), 2018. Miami, FL, USA, 17-19 December, doi:{10.1109/CDC.2018.8619019}.
18. Calafiore, G.; Polyak, B. Stochastic Algorithms for Exact and Approximate Feasibility of Robust LMIs. *IEEE Transactions on Automatic Control* **2001**, *46*, 1755–1759.
19. Nikoukhah, R.; Delebecque, F.; El Ghaoui, L. LMITOOL: a Package for LMI Optimization in Scilab User's Guide. Technical report, INRIA, RT-0170, ffinria-00070000, 1995.
20. Löfberg, J. YALMIP : A Toolbox for Modeling and Optimization in MATLAB. Procs. of the CACSD Conference; , 2004.
21. Eltved, A. Convex Relaxation Techniques for Nonlinear Optimization. PhD thesis, Technical University of Denmark, 2021.
22. Bi, Y. Analysis of Convex Relaxations for Nonconvex Optimization. PhD thesis, Cornell University, 2020.
23. Keller, A. Convex underestimating relaxation techniques for nonconvex polynomial programming problems: computational overview. *Journal of the Mechanical Behavior of Materials* **2015**, *24*, 129–143. https://doi.org/10.1515/jmbm-2015-0015.
24. Helton, J.; Klep, I.; McCullough, S. Relaxing LMI Domination Matricially. In Proceedings of the Procs. 49th IEEE Conference on Decision and Control (CDC), 2010. 15-17 December, Atlanta, GA, USA, https://doi.org/10.1109/CDC.2010.5717737.
25. Elizabeth, S.; Jothilakshmi, R. Convergence Analysis of Extended Kalman Filter in a Noisy Environment Through Difference Equations. *International Journal of Pure and Applied Mathematics* **2014**, *91*, 33–41.
26. Johnson, C.; Nylen, P. Monotonicity Properties of Norms. *Linear Algebra and its Applications* **1991**, *148*, 43–58.
27. Julier, S.; Uhlmann, J. Using covariance intersection for SLAM. *Robotics and Autonomous Systems* **2007**, *55*, 3—–20.

28. Chu, T.; Qi, G.; Li, Y.; Sheng, A. Distributed Asynchronous Fusion Algorithm for Sensor Networks with Packet Losses. *Discrete Dynamics in Nature and Society* **2014**, *2014*. https://doi.org/10.1155/2014/957439.
29. Wu, X.; Song, S. Covariance Intersection-based Fusion Algorithm for Asynchronous Multirate Multisensor System with Cross-correlation. *IET Science, Measurement & Technology* **2017**, *11*. https://doi.org/10.1049/iet-smt.2016.0524.